Nonlinear Control Applied in Jump Attenuation of a Non-ideal System

A. M. Tusset, A. Kossoski, A. M. Bueno, Jose Manoel Balthazar, J. L. P. Felix, A. Cunha Jr, and R. H. Avanço

Abstract This work proposes the attenuation of the Sommerfeld effect (jump phenomenon) present in a non-ideal oscillator thought the use of different nonlinear controllers. The non-ideal system is composed of a beam-like mechanical structure excited by a limited power supply, in this case an unbalanced direct current motor. Two different control techniques are considered. The first controller has its feedback gain obtained through the SDRE (State-Dependent Riccati Equation) technique in conjunction with a feedforward gain. The second controller is based in the SMC (Sliding Mode Control) technique. Numerical simulations show that the two proposed control strategies are effective in suppressing the jump phenomenon, and thus keeping the structure vibration of the studied system at desirable levels.

Keywords Non-ideal system · SDRE control · Sliding Mode Control · Sommerfeld effect

A. M. Tusset (✉)
Federal University of Technology, Paraná, Brazil

A. Kossoski · A. M. Bueno · J. M. Balthazar
Sao Paulo State University, São Paulo, Brazil
e-mail: atila.bueno@unesp.br

J. L. P. Felix
Federal University of Pampa, Rio Grande do Sul, Brazil
e-mail: jorge.felix@unipampa.edu.br

A. Cunha Jr
Rio de Janeiro State University, Rio de Janeiro, Brazil
e-mail: americo.cunha@uerj.br

R. H. Avanço
Federal University of Maranhão, Maranhão, Brazil

© The Author(s), under exclusive license to Springer Nature Switzerland AG 2022

J. M. Balthazar (ed.), *Nonlinear Vibrations Excited by Limited Power Sources*,
Mechanisms and Machine Science 116, https://doi.org/10.1007/978-3-030-96603-4_13

1 Introduction

The Sommerfeld effect is a resonance phenomenon that arises from the interaction between a non-ideal energy source with the mechanical structure. The energy source influences the mechanical structure, which in turn influences and exchanges energy with the source, in a two-way effect. The nomenclature of non-ideal energy source comes from the fact that the power supply provides limited energy to the system, thus being a characteristic of all real energy sources [1–6].

The first researcher who studied this phenomenon was Arnould Sommerfeld in 1902 [7]. Through a simple experiment, which consisted of an unbalanced DC electric motor fixed on a table, Sommerfeld realized that as the motor rotational speed approached the critical speed of the mechanical structure, the increase in voltage no longer corresponded to the increase in motor speed, but the vibration amplitudes continued to increase. This behavior was not expected, as direct current motors have their angular speed directly proportional to the armature voltage. Moreover, this behavior quickly changes when the system reaches a critical point, where the vibration amplitudes suddenly drop to low levels and the motor speed increases return to the values corresponding to the applied voltage, thus generating a jump phenomenon in the vibration amplitude graphs in relation to the motor angular velocity [2, 4, 8–10]

Some works have proposed methodologies to suppress the jump effect, because this effect if is unwanted as it represents a loss of system energy, as well as resulting in an amplification of the mechanical vibrations. Reference [11] proposed to include a friction element in a non-ideal structural system to eliminate the Sommerfeld effect. In [4] is considered a semi-active control using a magnetorheological damper for reducing the resonance vibrations of a non-ideal structure in an active way. Reference [12] considered a shape-memory alloy to attenuate the vibration and Sommerfeld effect of a non-ideal type oscillator. In [13] is considered a snap-through truss absorber for attenuation of the jump phenomenon in an oscillator under excitation of an electric motor with an eccentricity and limited power.

In this work is proposed the use of an active control in order to attenuate the Sommerfeld effect and the vibration amplitudes of a non-ideal mechanical oscillator. The NIS studied is composed of a beam and an unbalanced electric motor with limited power supply. For the active control of the system are considered two techniques. The first being a controller that uses a portion of feedback gain and another portion of feedforward gain and the second controller is based in the sliding mode control technique.

2 Mathematical Model

Figure 1a shows the mechanical part of the non-ideal system. In this figure, m_1 is the mass of the cart with the motor, m_2 is the motor unbalance mass, r is the length of the unbalance axis and φ is the position angle of the motor shaft. k and c represent

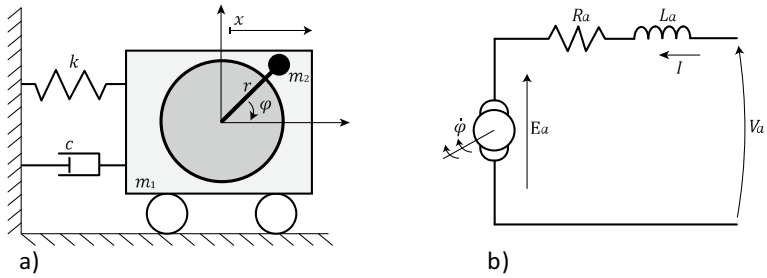

Fig. 1 **a** Non-ideal mechanical system (NIS). **b** electrical schematic representation of the DC motor

the stiffness and damping of the mechanical structure, respectively. Motor unbalance will cause vibration, with displacement x [4, 9, 14, 15].

The mathematical model that represents the dynamics of the system shown in Fig. 1 is developed using Lagrange's energy method, where the Lagrange's function is expressed as:

$$L = E_k - E_p \tag{1}$$

where E_k is the kinetic energy, and E_p is the potential energy. The equations of motion can be obtained through the Euler–Lagrange equation, given by:

$$\frac{d}{dt}\left(\frac{\partial L}{\partial \dot{Q}_i}\right) - \frac{\partial L}{\partial Q_i} = \Im_i \tag{2}$$

where i = 1, 2,..., N. N is the number of degrees-of-freedom, $\Im_i$'s are the non-conservatives forces, Q_i's are the generalized coordinates, being that $Q_1 = x$, and $Q_2 = \varphi$.

The kinetic energy is given by:

$$E_k = \frac{1}{2}m_1\dot{x}^2 + \frac{1}{2}J\dot{\varphi}^2 + \frac{1}{2}m_2\left((\dot{x} - \dot{\varphi}r\sin(\varphi))^2 + (\dot{\varphi}r\cos(\varphi))^2\right) \tag{3}$$

where: J is the moment of inertia, $\dot{\varphi}$ is the rotational speed, m_2 is the unbalanced mass.

The potential energy is given by:

$$E_p = \frac{1}{2}kx^2 \tag{4}$$

The non-conservatives forces are given by:

$$\Im_1 = -c\dot{x} \tag{5}$$

Substituting Eqs. (3), (4) into Eq. (1), and substituting the result accounting for Eq. (5) into Eq. (2), we obtain:

$$\begin{aligned} M\ddot{x} + c\dot{x} + kx &= mr(\dot{\varphi}^2 \sin(\varphi) + \ddot{\varphi}\cos(\varphi)) \\ (J + mr^2)\ddot{\varphi} &= mrx\cos(\ddot{\varphi}) + T_e \end{aligned} \tag{6}$$

where: $M = m_1 + m_2$

The electrical part, shown in Fig. 1b, refers to the circuit of a direct current motor. In this circuit, V_a is the applied armature voltage, I is the armature current. R_a and L_a are the resistance and inductance of the armature, respectively. E_A is the counter-electromotive force (CEMF) and in the case of constant flux can be directly related to the rotational speed of the motor as $E_a = k_e\dot{\varphi}$, where k_e is the electrical constant. Using the Kirchhoff's circuit laws will have:

$$V_a = R_a I + L_a \dot{I} + E_a \tag{7}$$

This is the voltage equation for the armature circuit of a DC motor. To obtain the motor torque equation, it is necessary to analyze its mechanical structure, where the torque experienced by the motor windings T_e can be directly related to the armature current as $T_e = k_t I$, where k_t is the torque constant. The equation of motion for a DC motor is given by:

$$T_e = J\ddot{\varphi} + b\dot{\varphi} + T_l \tag{8}$$

where: J is the inertia, b is the coefficient of viscous friction and T_l is the load torque. In this paper T_l will be neglected.

Coupling the elements of inertia, as well as relating the displacement of the mechanical structure to the angular displacement of the motor, it is possible to obtain the following set of equations, this being the set of dynamic nonlinear equations for the non-ideal system shown in Fig. 1.

$$\begin{aligned} M\ddot{x} + c\dot{x} + kx &= mr(\dot{\varphi}^2 \sin(\varphi) + \ddot{\varphi}\cos(\varphi)) \\ (J + mr^2)\ddot{\varphi} &= mrx\cos(\ddot{\varphi}) + k_t I \\ L_a \dot{I} &= R_a I - k_e I + V_a \end{aligned} \tag{9}$$

Equation (9) can be written in state-space notation as follows:

$$\begin{aligned} \dot{x}_1 &= x_2 \\ \dot{x}_2 &= \Delta\left(\alpha_1 x_5 \cos(x_3) - \alpha_2 x_4^2 \sin(x_3) - \alpha_3 x_2 - \alpha_4 x_1\right) \\ \dot{x}_3 &= x_4 \\ \dot{x}_4 &= \Delta\left(-\beta_1 x_4^2 \sin(x_3)\cos(x_3) - \beta_2 x_2 \cos(x_3) - b_3 x_1 \cos(x_3) + \beta_4 x_5\right) \end{aligned}$$

$$\dot{x}_5 = -c_1 x_5 - c_2 x_4 + c_3 \tag{10}$$

where: $x_1 = x$, $x_2 = \dot{x}$, $x_3 = \varphi$, $x_4 = \dot{\varphi}$, $x_5 = I$, $\alpha_1 = k_t mr$, $\alpha_2 = m^2 r^3 + Jmr$, $\alpha_3 = cmr^2 + cJ$, $\alpha_4 = kmr^2 + kJ$, $\alpha_5 = Mmr^2 + JM$, $\beta_1 = m^2 r^2$, $\beta_2 = cmr$, $\beta_3 = kmr$, $\beta_4 = Mk_t$, $c_1 = \frac{R_a}{L_a}$, $c_2 = \frac{k_e}{L_a}$, $c_3 = \frac{V}{L_a}$ and $\Delta = \frac{1}{-\beta_1 \cos(x_3)^2 + \alpha_5}$.

3 Numerical Simulations

The numerical simulations are carried out accounting for the following parameters: $m_1 = 0.13$, $m_2 = 0.005$, $k = 399$, $c = 0.077$, $t = 0.015$, $R_a = 51$, $J = 9 \times 10^{-7}$, $J = 2.82 \times 10^{-6}$, $L_a = 0.004$, $k_t = 0.0663$ and $k_m = 0.0663$.

Figure 2 shows the results for the jump phenomenon according to the motor shaft angular frequency and the voltage applied to the armature.

Considering the process of increasing the electrical voltage (V), the jump phenomenon occurs when the motor reaches 56 rad/s and 8.5 V. After this point, if the voltage increase is maintained, the system returns to the linear and normal operation expected. Due to the effect of the coupling between the motor and the

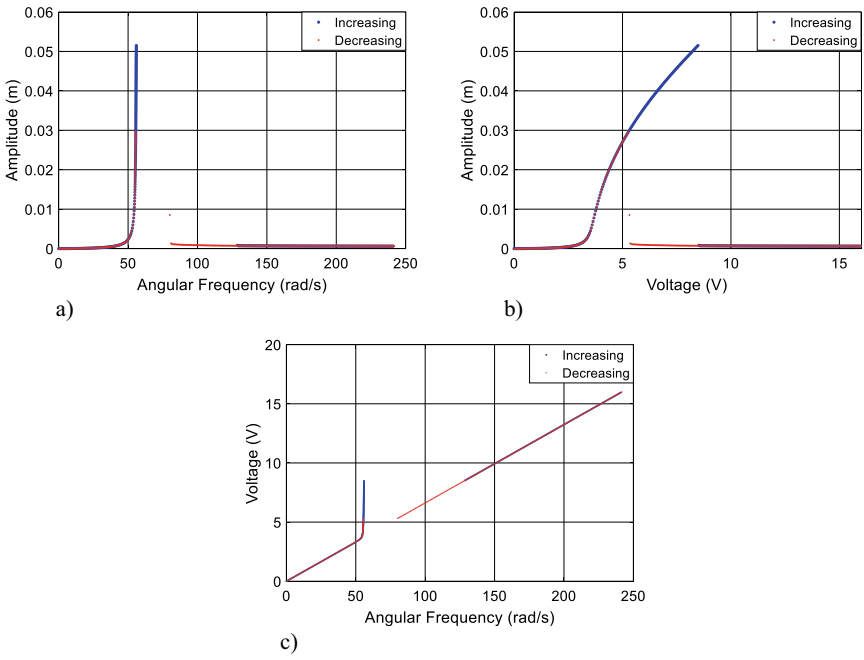

Fig. 2 Jump phenomenon. **a** Frequency response diagram. **b** Jump phenomenon due to the applied voltage in the DC motor. **c** Angular frequency response by voltage

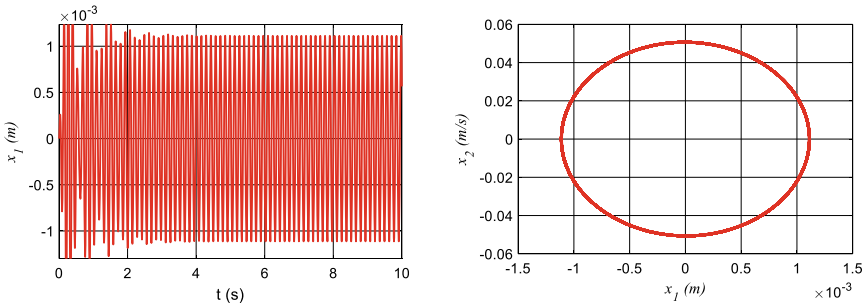

Fig. 3 Dynamics of the systems considering x_1. **a** Time history. **b** Phase plane for x_1 versus x_2

mechanical structure, the system has its operation weakened and it is realized that between 3.5 and 8.5 V all the increase of voltage in the motor serves almost solely to increase the amplitudes of vibration and not the rotation of the motor. This disruption of the direct relationship between electrical voltage and motor rotation can be clearly seen in Fig. 2c. The effect of converting electrical energy into mechanical vibration can also be observed during the process of decreasing the electrical voltage. However, as this is a non-linear system and that it depends on its initial conditions, the Sommerfeld effect of the voltage decrease process occurs at a different point than that of the increasing voltage process, in this case occurring when the motor reaches 55.5 rad/s and 5.3 V. This conversion of electrical energy into mechanical vibration energy is one of the biggest problems of this type of system, being responsible for reducing the efficiency of the electric motor, as well as reducing the angular frequencies available for the project.

In Fig. 3 it is possible to observe the behavior of the system (11), considering a voltage of 3 V applied to the DC motor.

As can be seen in Fig. 3, when the motor is powered with 3 V, the vibrations of the structure are low, showing a periodic behavior with a unit period after the transient period.

Considering the behavior of x_1 shown in Fig. 3, the following displacement equation for x_1 can be determined:

$$\begin{aligned} \tilde{x}_1 &= 0.001113 \sin(44.88t) \\ \tilde{x}_2 &= 0.05 \cos(44.88t) \end{aligned} \tag{11}$$

3.1 Nonlinear Control Project

Considering that the objective is to eliminate the Somerfield effect observed in x_1, the following control signal (U) can be introduced in Eq. (10) [9, 14, 16, 17]:

$$\begin{aligned}
\dot{x}_1 &= x_2 \\
\dot{x}_2 &= \Delta\left(\alpha_1 x_5 \cos(x_3) - \alpha_2 x_4^2 \sin(x_3) - \alpha_3 x_2 - \alpha_4 x_1\right) + U \\
\dot{x}_3 &= x_4 \\
\dot{x}_4 &= \Delta\left(-\beta_1 x_4^2 \sin(x_3)\cos(x_3) - \beta_2 x_2 \cos(x_3) - b_3 x_1 \cos(x_3) + \beta_4 x_5\right) \\
\dot{x}_5 &= -c_1 x_5 - c_2 x_4 + c_3
\end{aligned} \tag{12}$$

Since the objective of the control signal (U) is to control the displacement of x_1, the control design can be obtained by considering only the first two equations of (12). In addition, the states x_3, x_4 and x_5 will be considered disturbances in the system [9].

$$\begin{aligned}
\dot{x}_1 &= x_2 \\
\dot{x}_2 &= \Delta\left(\alpha_1 x_5 \cos(x_3) - \alpha_2 x_4^2 \sin(x_3) - \alpha_3 x_2 - \alpha_4 x_1\right) + U
\end{aligned} \tag{13}$$

3.2 Proposed SDRE Control

The vector control U for the Optimal Linear feedback control consists of two parts: $U = \tilde{u} + u$, where u is the optimal feedback control and $\tilde{u}$ is the feedforward control gain, the last one responsible for maintaining the system in the desired trajectory. The feedforward gain is given by:

$$\tilde{u} = -\Delta\left(\alpha_1 x_5 \cos(x_3) - \alpha_2 x_4^2 \sin(x_3) - \alpha_3 \tilde{x}_2 - \alpha_4 \tilde{x}_1\right) \tag{14}$$

Substituting Eq. (14) into Eq. (13), and defining the deviation of the desired trajectory as:

$$e = \begin{bmatrix} x_1 - \tilde{x}_1 \\ x_2 - \tilde{x}_2 \end{bmatrix} \tag{15}$$

where $\tilde{x}_1$ and $\tilde{x}_2$ are the trajectories desired. The system can be represented in the following form:

$$\begin{aligned}
\dot{e}_1 &= e_2 \\
\dot{e}_2 &= -\Delta\alpha_3 e_2 - \Delta\alpha_4 e_1 + u
\end{aligned} \tag{16}$$

Or in matrix form as:

$$\dot{\mathbf{e}} = \mathbf{Ae} + \mathbf{Bu} \tag{17}$$

The control $\boldsymbol{u}$ is optimal and it transfers the nonlinear system of Eq. (16) from any initial state to the final state $\mathbf{e}(\infty) = 0$.

Minimizing the cost functional to:

$$J = \int_0^\infty \left(\mathbf{e}^T\mathbf{Qe} + \mathbf{u}^T\mathbf{Ru}\right) dt \tag{18}$$

the control $\mathbf{u}$ can be found solving the following equation:

$$\mathbf{u} = -\mathbf{R}^{-1}\mathbf{B}^T\mathbf{Pe} \tag{19}$$

Being $\mathbf{P}$ a symmetric matrix, the Algebraic Riccati Equation is developed, denoted by:

$$\mathbf{PA} + \mathbf{A}^T\mathbf{P} - \mathbf{PBR}^{-1}\mathbf{B}^T\mathbf{P} + \mathbf{Q} = \mathbf{0} \tag{20}$$

The matrices $\mathbf{A}$ and $\mathbf{B}$ may be represented by: $\mathbf{A} = \begin{bmatrix} 0 & 1 \\ -\Delta\alpha_4 & -\Delta\alpha_3 \end{bmatrix}$, $\mathbf{B} = \begin{bmatrix} 0 \\ 1 \end{bmatrix}$ and by definition: $\mathbf{Q} = 10^4\begin{bmatrix} 10^3 & 0 \\ 0 & 1 \end{bmatrix}$ and $\mathbf{R} = 10^{-4}$.

In Figs. 4, it is observed the jump phenomenon suppression using the proposed control $U = \tilde{u} + u$, considering $\tilde{x}_1$ and $\tilde{x}_2$ obtained in the Eq. (11).

As can be seen in the results presented in Fig. 4, using the proposed control ($U = \tilde{u} + u$), it is possible to eliminate the jump effect, keeping the displacements in the desired amplitude and frequency.

3.3 Proposed Sliding Mode Control

For the sliding mode control, the sliding surface is generally given by [18, 19]:

$$s = e_2 + \lambda e_1 \tag{21}$$

The existence of the sliding mode requires the following conditions to be satisfied:

$$\begin{aligned} s &= e_2 + \lambda e_1 \\ \dot{s} &= \dot{e}_2 + \lambda e_1 \end{aligned} \tag{22}$$

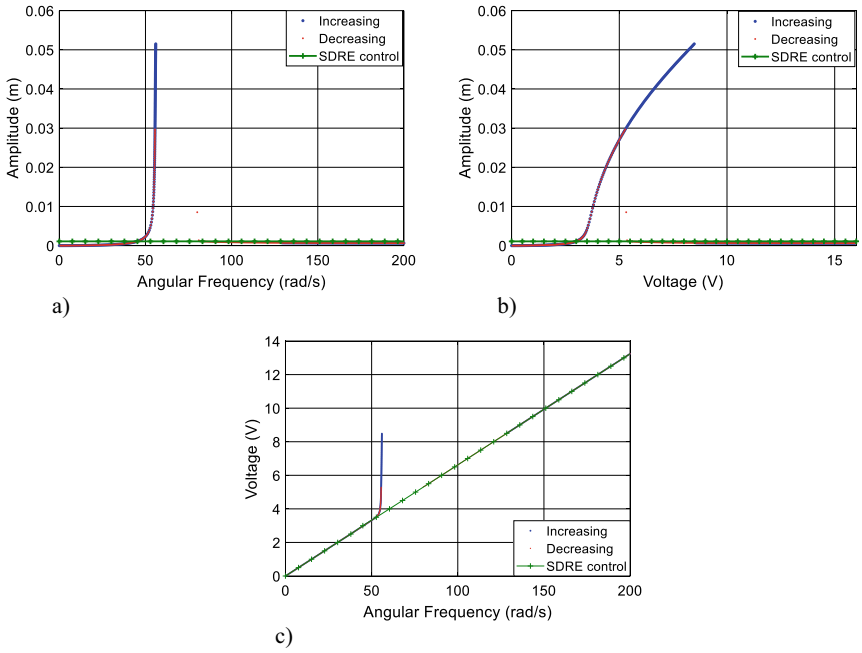

Fig. 4 Jump phenomenon suppression by SDRE control. **a** Frequency response diagram. **b** Jump phenomenon due to the applied voltage in the DC motor. **c** Angular frequency response by voltage

where λ represents a real number.

Equation (21) defines the output of the sliding mode control, while the reaching law is given by [18, 19]:

$$U = \begin{cases} U_{\max} & if \quad \frac{s}{\mu} < -1 \\ -U_{\max} & if \quad \frac{s}{\mu} > 1 \\ K_{smc}s \;\; if & -1 < \frac{s}{\mu} < 1 \end{cases} \tag{23}$$

where μ is the layer thickness of the control, K_{smc} is a proportional gain, and $U_{\max}$ is related to the saturation value. The parameters μ and K_{smc} are positive constants [18, 19].

In Figs. 5, it is observed the jump phenomenon suppression using the Proposed sliding mode control for parameters: $\mu = 10^{-3}$, $K_{smc} = 10^3$ and $U_{\max} = 100$.

It can be seen in Fig. 5 that the proposed control using the sliding mode control was also efficient in suppressing the jump effect, keeping the displacements in the desired amplitude and frequency.

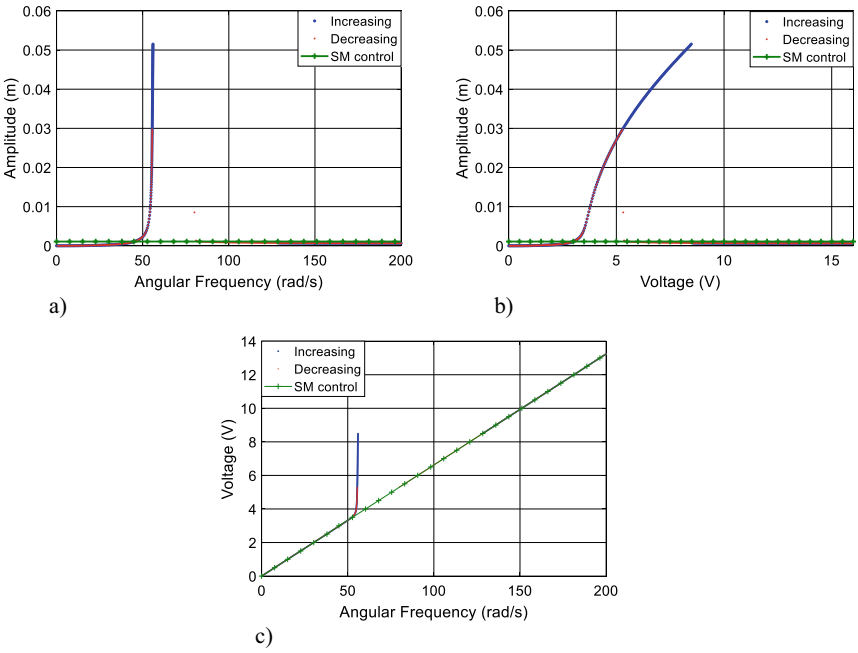

Fig. 5 Jump phenomenon suppression by Sliding Mode control. **a** Frequency response diagram. **b** Jump phenomenon due to the applied voltage in the DC motor. **c** Angular frequency response by voltage

4 Conclusions

This work presented two control techniques for suppression of the Sommerfeld effect of a non-ideal system, i.e., a system where the excitation source is influenced by its own performance, losing energy in the process that serves only to amplify the vibration amplitudes.

The numerical results showed that both the SDRE and SMC controls are efficient in suppressing the jump effect, keeping the vibration amplitudes at desired levels as well as the motor voltage.

References

1. Kononenko, V.O.: Vibrating System of Limited Power Supply. Illife Books, London (1969)
2. Nayfeh, A.H., Mook, D.T.: Nonlinear Oscillations. Wiley-Interscience, New York (1979)
3. Krasnopolskaya, T.S.: Chaos in acoustic subspace raised by the Sommerfeld-Kononenko effect. Meccanica **41**, 299–310 (2006)
4. Piccirillo, V., Tusset, A.M., Balthazar, J.M.: Dynamical jump attenuation in a non-ideal system through magneto rheological damper. J. Theor. Appl. Mech. **53**, 595–604 (2014)

5. Gonçalves, P.J.P., Silveira, M., Petronio, E.A., Pontes, B.R., Balthazar, J.M.: Double resonance capture of a two-degree-of-freedom oscillator coupled to a non-ideal motor. Meccanica **51**, 2203–2214 (2016)
6. Balthazar J. M., Tusset A. M., Brasil R. M. L. R. F., Felix J. L. P., Rocha R. T., Janzen, F. C., Nabarrete, A., Oliveira C.: An overview on the appearance of the Sommerfeld effect and saturation phenomenon in non-ideal vibrating systems (NIS) in macro and MEMS scales. Nonlinear Dyn. **93**, 19–40 (2018)
7. Sommerfeld, A.: Beiträge zum dynamischen ausbau der festigkeitslehe. Phys. Z. **3**, 266–286 (1902)
8. Tusset, A.M., Balthazar, J.M.: On the chaotic suppression of both ideal and non-ideal duffing based vibrating systems, using a magnetorheological damper. Differ. Equ. Dyn. Syst. **21**, 105–121 (2013)
9. Tusset A.M., Piccirillo V., Balthazar J.M., Brasil M.R.L.F.: On suppression of chaotic motions of a portal frame structure under non-ideal loading using a magneto-rheological damper. J. Theoret. Appl. Mech., 653–664 (2015)
10. Awrejcewicz, J., Starosta, R., Sypniewska-Kaminska, G.: Decomposition of governing equations in the analysis of resonant response of a nonlinear and non-ideal vibrating. Nonlinear Dyn. **82**, 299–309 (2015)
11. Felix, J.L.P., Balthazar, J.M., Brasil, R.M.L.R.F., Pontes, B.R.: On lugre friction model to mitigate Nonideal vibrations. ASME. J. Comput. Nonlinear Dynam. **4**, 034503 (2009)
12. Kossoski, A., Tusset, A.M., Janzen, F.C., Rocha, R.T., Balthazar, J.M., Brasil, R.M.L.R.F., Nabarrete, A.: Jump attenuation in a non-ideal system using shape memory element. Matec Web Conf. **148**, 03003–03003–4 (2018)
13. De Godoy, W.R., Balthazar, J.M., Pontes, B.R., Felix, J.L., Tusset, A.M.: A note on non-linear phenomena in a non-ideal oscillator, with a snap-through truss absorber, including parameter uncertainties. Proc. Inst. Mech. Eng. Part K: J. Multi-body Dyn. **227**, 76–86 (2013)
14. Tusset, A.M., Balthazar, J.M., Rocha, R.T., Ribeiro, M.A., Lenz, W.B., Janzen, F.C.: Time-Delayed Feedback Control Applied in a Nonideal System with Chaotic Behavior. Nonlinear Dynamics and Control. 1ed.: Springer International Publishing, Vol. 1, pp. 237–244 (2020)
15. Kossoski, A., Tusset, A.M., Janzen, F.C., Ribeiro, M.A., Balthazar, J.M.: Attenuation of the Vibration in a Non-ideal Excited Flexible Electromechanical System Using a Shape Memory Alloy Actuator. Mechanisms and Machine Science. 1ed.: Springer International Publishing, Vol. 95, pp. 431–444 (2021)
16. Tusset, A.M., Balthazar, J.M., Chavarette, F.R., Felix, J.L.P.: On energy transfer phenomena, in a nonlinear ideal and nonideal essential vibrating systems, coupled to a (MR) magneto-rheological damper. Nonlinear Dyn. **69**, 1859–1880 (2012)
17. Tusset, A.M., Balthazar, J.M., Felix, J.L.P.: On elimination of chaotic behavior in a non-ideal portal frame structural system, using both passive and active controls. J. Vib. Control **19**, 803–813 (2013)
18. Bassinello, D.G., Tusset, A.M., Rocha, R.T., Balthazar, J.M.: Dynamical analysis and control of a chaotic microelectromechanical resonator model. Shock. Vib. **50**, 1–10 (2018)
19. Piccirillo, V., Goes, L.C.S., Balthazar, J.M., Tusset, A.M.: Deflection control of an aeroelastic system utilizing an antagonistic shape memory alloy actuator. Meccanica **53**, 727–745 (2017)